

# Journal of Materials Chemistry B

Accepted Manuscript



This is an *Accepted Manuscript*, which has been through the Royal Society of Chemistry peer review process and has been accepted for publication.

*Accepted Manuscripts* are published online shortly after acceptance, before technical editing, formatting and proof reading. Using this free service, authors can make their results available to the community, in citable form, before we publish the edited article. We will replace this *Accepted Manuscript* with the edited and formatted *Advance Article* as soon as it is available.

You can find more information about *Accepted Manuscripts* in the [Information for Authors](#).

Please note that technical editing may introduce minor changes to the text and/or graphics, which may alter content. The journal's standard [Terms & Conditions](#) and the [Ethical guidelines](#) still apply. In no event shall the Royal Society of Chemistry be held responsible for any errors or omissions in this *Accepted Manuscript* or any consequences arising from the use of any information it contains.

## ARTICLE

## Phase transformation from hydroxyapatite to the secondary bone mineral, whitlockite

Cite this: DOI: 10.1039/x0xx00000x

Hae Lin Jang, Hye Kyoung Lee, Kyongsuk Jin, Hyo-Yong Ahn, Hye-Eun Lee and Ki Tae Nam

Received 00th January 2012.  
Accepted 00th January 2012

DOI: 10.1039/x0xx00000x

www.rsc.org/

Whitlockite (WH:  $\text{Ca}_{18}\text{Mg}_2(\text{HPO}_4)_2(\text{PO}_4)_{12}$ ) is the second most abundant mineral in hard tissue, but its precipitation mechanism or role in the body system is poorly understood. Here, using a newly discovered synthetic method for WH, we investigated the kinetic mechanism for the precipitation of WH in physiologically similar conditions, excluding any effects of the toxic ions. Based on systematically classified stages in the precipitation process of WH, we monitored the transformation of calcium phosphate phases from neutral pH to acidic pH with the addition of  $\text{H}_3\text{PO}_4$ . The study revealed that at 70 °C, hydroxyapatite (HAP:  $\text{Ca}_{10}(\text{PO}_4)_6(\text{OH})_2$ ) transforms into dicalcium phosphate dehydrate (DCPD:  $\text{CaHPO}_4 \cdot 2\text{H}_2\text{O}$ ) and then into WH in the presence of  $\text{Mg}^{2+}$  ions as the pH decreases. The transformation process involves the multiple intermediates, of which the stability depends on the cation (Ca and Mg) activities and the solution pH. WH is the most stable calcium phosphate compound below pH 4.2, whereas HAP is the most stable around neutral pH. We also found that  $\text{Mg}^{2+}$  ions, which are known to block the growth of HAP, can play a key role in WH formation. This study provides new insight into the interplay of biologically important calcium phosphate compounds.

### Introduction

The two most abundant biominerals in hard tissues are hydroxyapatite (HAP:  $\text{Ca}_{10}(\text{PO}_4)_6(\text{OH})_2$ ) and whitlockite (WH:  $\text{Ca}_{18}\text{Mg}_2(\text{HPO}_4)_2(\text{PO}_4)_{12}$ ).<sup>1-6</sup> Although HAP is the major phase of hard tissue, a short-range ordered WH phase in an amorphous form also exists in human bone and dentin with an estimated amount of approximately 20 wt% and 26 to 58 wt%, respectively, based on the amount of Mg.<sup>1</sup> Notably, a higher ratio of WH exists in the younger-aged body<sup>7</sup> and in the earlier stage of biomineralization,<sup>8</sup> which indicates that WH has important influences in the development of hard tissue. Although HAP has been actively investigated, remarkably little is still known about the role and the precipitation mechanism of WH due to the difficulty of its synthesis.

Recently, a new synthetic method of WH was developed in a ternary  $\text{Ca}(\text{OH})_2$ - $\text{Mg}(\text{OH})_2$ - $\text{H}_3\text{PO}_4$  aqueous system.<sup>9</sup> Pure-phase WH nanoparticles were obtained in an acidic condition with excess  $\text{Mg}^{2+}$  ions, where precipitation of HAP was impeded. Especially, synthesized WH was clearly distinguished from its synthetically analogous tricalcium phosphate (TCP:  $\text{Ca}_3(\text{PO}_4)_2$ ) due to the existence of the  $\text{HPO}_4^{2-}$  group. When fabricated into cellular scaffolds, WH showed better biocompatibility than HAP and TCP, based on the proliferation level of human bone cells and their RNA expression level related to bone mineralization. In addition, interestingly, the solubility test revealed that WH had a greater stability than HAP in acidic conditions below pH 4.2. The different stabilities of WH and HAP according to the pH suggest that WH might be

generated from a different precipitation mechanism than HAP in vivo. Therefore, revealing the formation mechanism of WH can allow us to comprehend the role of WH in the living system and thus the nature of bone *per se*. Here, we investigated the kinetic mechanism during WH precipitation in a ternary  $\text{Ca}(\text{OH})_2$ - $\text{Mg}(\text{OH})_2$ - $\text{H}_3\text{PO}_4$  aqueous system to mimic physiological conditions at a basic level, by preventing any interruption of the toxic ions such as  $\text{NO}_3^-$ ,  $\text{Cl}^-$  and  $\text{SO}_4^{2-}$ .

The WH phase can be precipitated with the support of secondary ions, such as  $\text{Mg}^{2+}$ ,  $\text{Co}^{2+}$ ,  $\text{Mn}^{2+}$ ,  $\text{Fe}^{2+}$ ,  $\text{Ni}^{2+}$  or  $\text{Zn}^{2+}$ .<sup>1, 2, 10-14</sup> Notably,  $\text{Mg}^{2+}$  has been reported to inhibit the formation or crystallization of dicalcium phosphate dehydrate (DCPD:  $\text{CaHPO}_4 \cdot 2\text{H}_2\text{O}$ ), octacalcium phosphate (OCP:  $\text{Ca}_8(\text{HPO}_4)_2(\text{PO}_4)_4 \cdot 5\text{H}_2\text{O}$ ) and HAP. For example,  $\text{Mg}^{2+}$  retards the growth of DCPD and OCP by adsorbing at their crystal surface and disturbing their atomic arrangement.<sup>1, 15, 16</sup> The growth of HAP is also impeded by  $\text{Mg}^{2+}$  because these ions block active growth sites and interrupt the crystal structure.<sup>1, 17, 18</sup> In contrast, in the presence of  $\text{Mg}^{2+}$ , it has been reported that the heterogeneous phase of WH can be obtained from starting materials such as DCPD and dicalcium phosphate anhydrate (DCPA:  $\text{CaHPO}_4$ ), under certain experimental acidic conditions.<sup>1, 2, 10, 12</sup> However, to the best of our knowledge, there have been no systematic studies investigating the kinetic mechanism for the precipitation of WH in the Ca-Mg-P aqueous system that exclude other effects of ions.

In this study, we identified five different intermediate stages during the transformation of HAP to WH by monitoring the pH change. Because the drops of  $\text{H}_3\text{PO}_4$  solution were added

continuously, the consistent decrease of pH was expected. However, as different phases formed at different pH levels, the region where the pH was maintained could be observed. Thus, from each stage, we collected intermediate precipitants and analyzed the kinetic precipitation pathway of WH and found that it consisted of a series of phase transformation processes to form a more stabilized phase. Based on the finding that WH is one of the most thermodynamically stable Mg-incorporated calcium phosphate compounds in acidic conditions, we also confirmed that HAP can directly transform into WH under proper acidic pH conditions with a sufficient amount of  $Mg^{2+}$  ions.

## Results and discussion

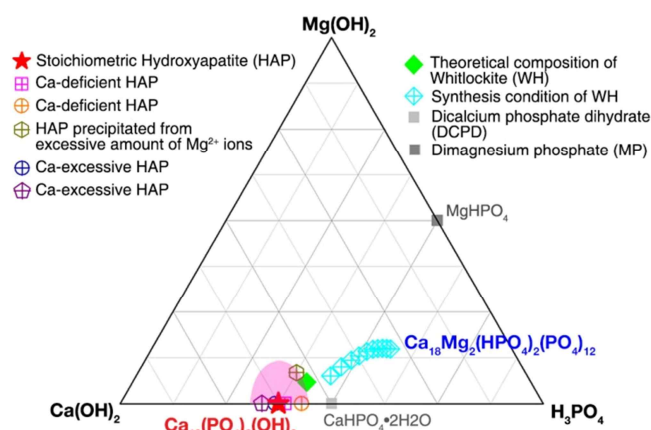


**Figure 1.** Precipitation conditions of whitlockite (WH:  $Ca_{18}Mg_2(HPO_4)_2(PO_4)_{12}$ ) and hydroxyapatite (HAP:  $Ca_{10}(PO_4)_6(OH)_2$ ), the two major bone minerals. The precipitation conditions of WH,<sup>9</sup> stoichiometric HAP,  $Ca^{2+}$ -deficient nonstoichiometric HAP,<sup>19, 20</sup>  $Ca^{2+}$ -excessive nonstoichiometric HAP<sup>21, 22</sup> and nonstoichiometric HAP with excess amounts of  $Mg^{2+}$  ions<sup>23</sup> are shown in the ternary  $Ca(OH)_2$ - $Mg(OH)_2$ - $H_3PO_4$  diagram. Although the theoretical composition of WH (green diamond) locates in the nonstoichiometric HAP precipitation region (magenta region), pure WH (blue diamond) precipitates in acidic conditions with an excess amount of  $Mg^{2+}$  ions.

To present the precipitation conditions of two major biominerals, HAP and WH, we indicated the synthesis conditions of HAP, nonstoichiometric HAP and WH on the ternary  $Ca(OH)_2$ - $Mg(OH)_2$ - $H_3PO_4$  diagram (Figure 1). Although the pure phase of HAP precipitated in accordance with its compositional molar ratio of Ca:P = 10:6, WH did not precipitate according to its theoretical compositional molar ratio (Ca:Mg:P = 18:2:14). Thus, we confirmed the previously considered notion that WH is difficult to synthesize. Instead, HAP was precipitated as a major phase when Ca, Mg and P were mixed depending on the theoretical ratio of WH. This result is due to the fact that HAP is thermodynamically the most stable calcium phosphate compound in the neutral pH region<sup>24</sup> and is a nonstoichiometric compound that can accept a wide range of atomic disorder in its flexible lattice.<sup>19</sup> In fact, in Figure 1, we can see that the theoretical composition of WH (green diamond) is located near the precipitation region of nonstoichiometric HAP (magenta region). However, we recently revealed that a pure phase of WH can precipitate in acidic conditions with an excess amount of  $Mg^{2+}$  because the

stability of WH exceeds that of HAP.<sup>9</sup> For example, a pure phase of WH can be synthesized by mixing the starting materials in a molar ratio of Ca:Mg:P = 0.39:0.12:0.49%. The possible synthesis conditions of WH, which we experimentally verified, are indicated by the blue diamonds in Figure 1.

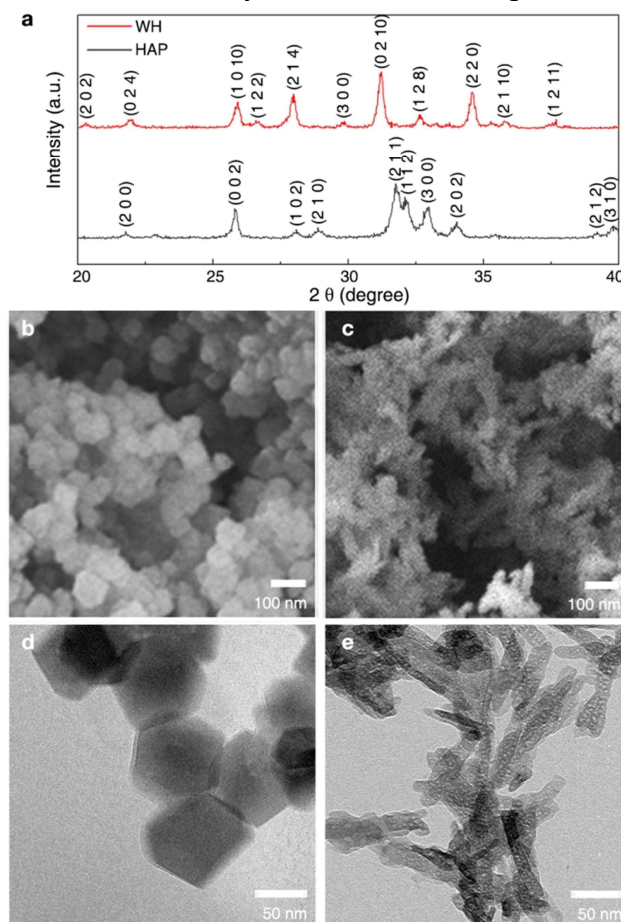


**Figure 2.** Synthesized whitlockite (WH:  $Ca_{18}Mg_2(HPO_4)_2(PO_4)_{12}$ ) nanoparticles and hydroxyapatite (HAP:  $Ca_{10}(PO_4)_6(OH)_2$ ) nanoparticles. (a) X-ray diffraction patterns of the synthesized WH and HAP, confirming that pure phases were formed. (b) Field emission scanning electron microscopy (FESEM) image of homogeneous WH nanoparticles with a size of approximately 50 nm. (c) FESEM image of homogeneous HAP nanoparticles with a size of approximately 80 nm. (d) HRTEM image of WH nanoparticles with a rhombohedral morphology. (e) HRTEM image of HAP nanoparticles with a rice shape.

Based on the newly discovered precipitation conditions for WH, we synthesized WH nanoparticles by adding 500 mL of 0.95 M  $H_3PO_4$  dropwise into a 500 mL aqueous solution of 0.77 M  $Ca(OH)_2$  and 0.23 M  $Mg(OH)_2$  using a digital burette. The solutions were vigorously stirred to achieve homogeneous mixing and maintained at 70 °C for rapid reaction. To directly compare WH and HAP, we also synthesized stoichiometric HAP using a sonochemistry based precipitation method. According to the theoretical composition ratio of HAP, 500 mL of a 0.6 M  $H_3PO_4$  aqueous solution was added dropwise into a 500 mL solution of 1.0 M  $Ca(OH)_2$ . Sonication was provided during the entire reaction to completely mix all of the starting materials and avoid precipitations of nonstoichiometric HAP. After drying, the pH of HAP was measured to be approximately

7 in distilled water, confirming its electroneutrality based on its stoichiometric phase. Using X-ray diffraction analysis, we confirmed that the synthesized WH had a homogeneous phase without any trace of HAP (Figure 2a). From the field emission scanning electron microscopy (FESEM) images, we observed that the WH and HAP nanoparticles had homogeneous sizes of approximately 50 nm (Figure 2b) and 80 nm (Figure 2c), respectively. In addition, from the high-resolution TEM observation, the WH and HAP nanoparticles had rhombohedral morphologies (Figure 2d) and rice shapes (Figure 2e), respectively.

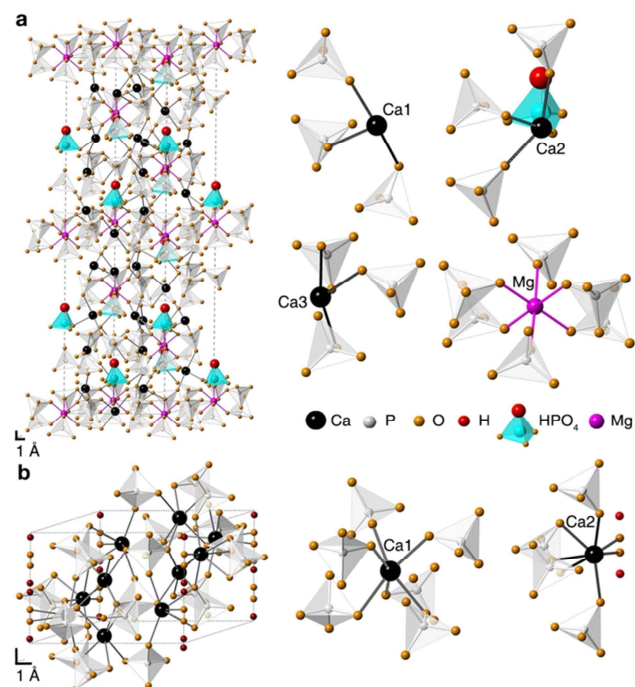


**Figure 3.** Atomic arrangements in the whitlockite (WH:  $\text{Ca}_{18}\text{Mg}_2(\text{HPO}_4)_2(\text{PO}_4)_{12}$ ) unit cell and the hydroxyapatite (HAP:  $\text{Ca}_{10}(\text{PO}_4)_6(\text{OH})_2$ ) unit cell. (a) Unit cell of WH and enlarged images of different calcium and magnesium sites in WH with surrounding phosphate groups. (b) Unit cell of HAP and enlarged images of different calcium sites in HAP with surrounding phosphate groups. The sizes of the major atoms are exaggerated for easier observation.

Despite the frequent simultaneous occurrence of WH and HAP in biominerals,<sup>1-6</sup> the atomic arrangements of the WH (rhombohedral ( $R\bar{3}c$ ) structure)<sup>2, 25</sup> and the HAP (hexagonal ( $P63/m$ ) structure)<sup>2</sup> are significantly different. To directly compare the atomic arrangements in the WH and HAP structures, we presented the unit cell of WH in a hexagonal setting with its lattice constants as  $a = 10.350 \text{ \AA}$  and  $c = 37.085 \text{ \AA}$  (Figure 3a).<sup>2</sup> The atomic arrangement of WH belongs to a general  $\text{Ba}_3\text{P}_2\text{O}_8$  structural type in which two types of atomic columns periodically repeat: 1) Ca1- $\text{PO}_4$ - $\text{PO}_4$ -Ca2-Ca3 and 2) Mg- $\text{HPO}_4$ .<sup>2, 9, 25</sup> Based on the unit cell of WH, we showed magnified images from different calcium (Ca1, Ca2 and Ca3) and magnesium (Mg) sites with their neighboring phosphate groups. The Ca1 atom was directly bonded to three phosphate groups, which were in the  $\text{PO}_4^{3-}$  form. One of these  $\text{PO}_4^{3-}$  groups was also directly connected with a Mg atom. The Mg<sup>2+</sup> ion had six surrounding  $\text{PO}_4^{3-}$  groups. The Ca2 atom was directly surrounded by  $\text{HPO}_4^{2-}$  with three  $\text{PO}_4^{3-}$  groups. The Ca3 atom had three neighboring  $\text{PO}_4^{3-}$  groups. However, the

hexagonal structure of HAP had lattice constants of  $a = 9.4176 \text{ \AA}$ ,  $c = 6.8814 \text{ \AA}$  and showed a different overall feature compared with WH, as shown in Figure 3b. WH had a higher packing density normal to the  $c$  axis than HAP due to the strong binding between Ca and P across the edge region.<sup>25</sup> Even though the  $\text{PO}_4^{3-}$  groups surrounding the Ca1 site in HAP appeared similar to the Mg site in WH, it is known that HAP crystal structure can hardly adopt  $\text{Mg}^{2+}$  due to the small atomic size of  $\text{Mg}^{2+}$ .<sup>1, 26</sup> In addition, the Ca2 site has four surrounding  $\text{PO}_4^{3-}$  groups and two OH<sup>-</sup> groups, which makes its atomic arrangement completely different than WH.

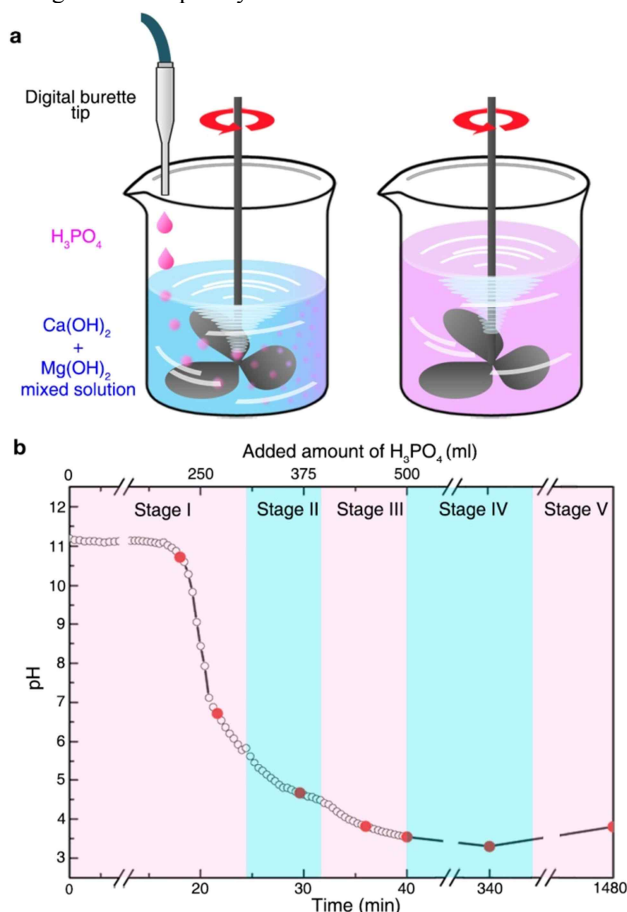


**Figure 4.** pH change during the precipitation of whitlockite (WH:  $\text{Ca}_{18}\text{Mg}_2(\text{HPO}_4)_2(\text{PO}_4)_{12}$ ). (a) Experimental set-up for synthesizing WH. Phosphoric acid ( $\text{H}_3\text{PO}_4$ , 0.95 M, 500 mL) was added dropwise into 500 mL of the mixed solution of 0.77 M calcium hydroxide ( $\text{Ca}(\text{OH})_2$ ) and 0.23 M magnesium hydroxide ( $\text{Mg}(\text{OH})_2$ ) using a digital burette. The solution was vigorously stirred to homogeneously mix all of the components. (b) The pH change from basic to acidic in the synthesis system of WH. Based on the different inclination level of pH decrease, we classified the kinetic precipitation pathway of WH into five stages to analyze its intermediate phases. We collected and analyzed intermediate precipitant from each stage (red circle) during the reaction when 225 mL, 270 mL, 370 mL and 450 mL of  $\text{H}_3\text{PO}_4$  were added to the  $\text{Ca}(\text{OH})_2$  and  $\text{Mg}(\text{OH})_2$  system and after the reaction when the aging time was 1 minute, 4 hour, 5 hour and 24 hour.

To investigate the formation mechanism of WH, we experimentally observed the kinetic precipitation pathway of WH. To precipitate a pure phase of WH, we added a  $\text{H}_3\text{PO}_4$

solution dropwise into an aqueous solution of  $\text{Ca}(\text{OH})_2$  and  $\text{Mg}(\text{OH})_2$ , which was stirred vigorously to achieve a homogeneous reaction (Figure 4a). As a result, the pH of the system dramatically changed from basic to acidic. Thus, we hypothesized that an initial phase of calcium phosphate compounds may have existed, which was stable in the basic conditions and later transformed into another stable phase in the acidic conditions. Interestingly, even though we added  $\text{H}_3\text{PO}_4$  droplets into a mixed solution of  $\text{Ca}(\text{OH})_2$  and  $\text{Mg}(\text{OH})_2$  with a constant velocity of 12.5 mL/min, different gradient levels throughout the pH decrease existed when we monitored the pH of the system. Initially, the pH of the 0.77 M  $\text{Ca}(\text{OH})_2$  and 0.23 M  $\text{Mg}(\text{OH})_2$  mixed aqueous solution was measured to be 11.2. When less than 225 mL of 0.95 M  $\text{H}_3\text{PO}_4$  was added to the  $\text{Ca}(\text{OH})_2$ - $\text{Mg}(\text{OH})_2$  solution, the system constantly maintained its pH level. After 225 mL and 305 mL of  $\text{H}_3\text{PO}_4$  were added, the pH of the system rapidly decreased from 10.7 to 5.8, and the gradient of pH slope turned relatively low at the end. As more  $\text{H}_3\text{PO}_4$  was added into the system, from 305 mL to 390 mL, the pH of the system sharply decreased again from 5.8 to 4.5. Similarly, a relatively slow pH decrease tendency existed at the end of the stage. The decrease in pH became rapid again when the added amount of  $\text{H}_3\text{PO}_4$  was 390 mL. The pH of the system changed from 4.5 to 3.5 when the 500 mL of  $\text{H}_3\text{PO}_4$  was added.

These different pH changes indicated formation of various intermediate phases, which consumed  $\text{H}_3\text{PO}_4$  at different pH levels. The pH of the system should have been maintained when the cations continuously reacted with newly incorporated  $\text{H}_3\text{PO}_4$  and precipitated into an intermediate phase. After the cations were all consumed at a certain pH level, additional  $\text{H}_3\text{PO}_4$  may have rapidly lowered the pH level of the system. The decreased pH of the system made the previous intermediate phase unstable. Thus, the next intermediate phase with a higher stability should have been generated by reacting with additionally incorporated  $\text{H}_3\text{PO}_4$  in the system.

To analyze the intermediate phases of WH, we divided the precipitation process into sequential stages according to the different levels of inclination to pH decrease and collected intermediate precipitants from each stage. We assigned the stages from I to III to the conditions where 0 mL ~ 305 mL, 305 mL ~ 390 mL and 390 mL ~ 500 mL of  $\text{H}_3\text{PO}_4$  were added into the system. During these stages, the pH of the system changed from 11.2 to 5.8, 5.8 to 4.5 and 4.5 to 3.5, respectively. After the addition of  $\text{H}_3\text{PO}_4$  was complete, the pH of the system changed to approximately 3.3 (stage IV) and slightly increased to 3.7 (stage V) with aging times of 5 hours and 24 hours, respectively, reflecting the existence of different phases.

In Figure 5a, we analyzed the X-ray diffraction patterns of the intermediate phases formed during the precipitation of WH at 70 °C. At stage I, HAP and  $\text{Mg}(\text{OH})_2$  were the major phases of the collected precipitant, which meant that  $\text{Ca}(\text{OH})_2$  preferentially reacted with  $\text{H}_3\text{PO}_4$  and produced HAP while  $\text{Mg}(\text{OH})_2$  remained ( $k'_{\text{Ca}(\text{OH})_2} = 5.5 \times 10^{-6}$ ,  $k'_{\text{Mg}(\text{OH})_2} = 1.8 \times 10^{-11}$ ).<sup>27</sup> At stage II, when the  $\text{Ca}(\text{OH})_2$  was almost consumed,  $\text{Mg}(\text{OH})_2$  began reacting with  $\text{H}_3\text{PO}_4$  because  $\text{Mg}(\text{OH})_2$  was less stable than HAP ( $k'_{\text{HAP}} = 3.04 \times 10^{-59}$ ).<sup>28</sup> As a result, the XRD peaks of  $\text{Mg}(\text{OH})_2$  disappeared. Instead, XRD peaks of dimagnesium phosphate (MP:  $\text{MgHPO}_4 \cdot x\text{H}_2\text{O}$ ) clearly appeared. Then, as the system became more acidic due to the continuous addition of  $\text{H}_3\text{PO}_4$  at stage III, HAP became unstable and partially changed into dicalcium phosphate dihydrate (DCPD:  $\text{CaHPO}_4 \cdot 2\text{H}_2\text{O}$ ), which is the kinetically favored phase of calcium phosphate in acidic conditions.<sup>2</sup>

Immediately after the complete addition of the total amount of  $\text{H}_3\text{PO}_4$ , the major phases were found to be HAP, DCPD and MP. At stage IV, during aging in the acidic system of pH 3.3, HAP gradually dissolved and thus its XRD peak intensity decreased. Additionally, the XRD peaks of DCPD and MP almost disappeared. In contrast, within aging time of 5 hours, the XRD peak intensities of the WH phase clearly increased. Finally, at stage V when the aging time was 24 hours, the XRD peaks of residual HAP completely disappeared and only a pure phase of WH was observed. During the transition from stage IV to V, the pH of the system slightly increased from 3.3 to 3.7 as the ratio between cation and anion ( $(\text{Ca}+\text{Mg})/\text{P}$ ) of dominant precipitant decreased.

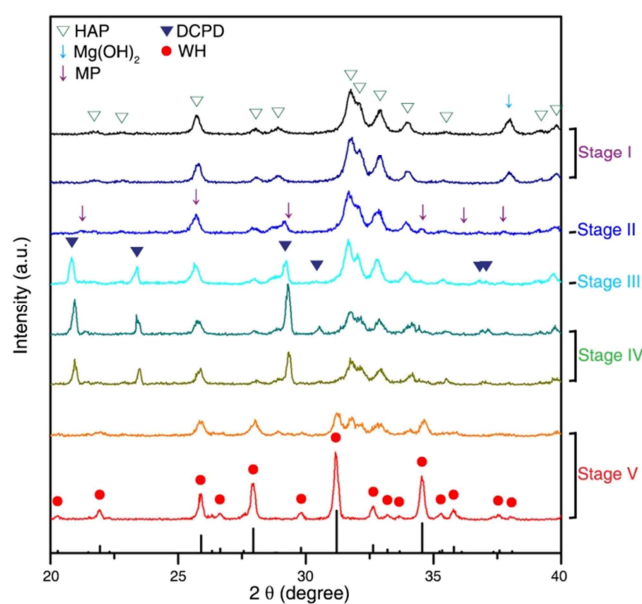


**Figure 5.** X-ray diffraction analysis of intermediate precipitants collected during the synthesis of whitlockite (WH:  $\text{Ca}_{18}\text{Mg}_2(\text{HPO}_4)_2(\text{PO}_4)_{12}$ ). Peaks corresponding to each phase of hydroxyapatite (HAP:  $\text{Ca}_{10}(\text{PO}_4)_6(\text{OH})_2$ ), magnesium hydroxide ( $\text{Mg}(\text{OH})_2$ ), magnesium phosphate (MP:  $\text{MgHPO}_4$ ), dicalcium phosphate dihydrate (DCPD:  $\text{CaHPO}_4 \cdot 2\text{H}_2\text{O}$ ) and WH in XRD data are marked as green triangle, cyan arrow, purple arrow, navy triangle and red circle, respectively. Additionally, reference peaks of WH from JCPDS No. 70-2064 are shown at the bottom.

The morphologies of the precipitants collected at different experimental times also showed the intermediate phases formed during the precipitation of WH. We observed the precipitants collected from different stages using FESEM. In stage I of WH precipitation at 70 °C (Figure 6a), rice shaped HAP nanoparticles were observed, which were transformed from  $\text{Ca}(\text{OH})_2$  particles, whereas polygonal platelet morphologies of  $\text{Mg}(\text{OH})_2$  nanoparticles remained (marked by yellow arrows).<sup>29</sup> At stage II (Figure 6b), the  $\text{Mg}(\text{OH})_2$  nanoparticles were dissolved and transformed into the cuboid form of MP, which were on the micrometer scale. On the surface of the MP, rice shaped HAP nanoparticles still existed. However, when the pH of the system decreased, a portion of the HAP nanoparticles were dissolved and large platelet shaped micrometer-size DCPD appeared, as shown in Figure 6c. On the surface of the DCPD, HAP nanoparticles still remained. During the aging process after the total amount of  $\text{H}_3\text{PO}_4$  was added into the

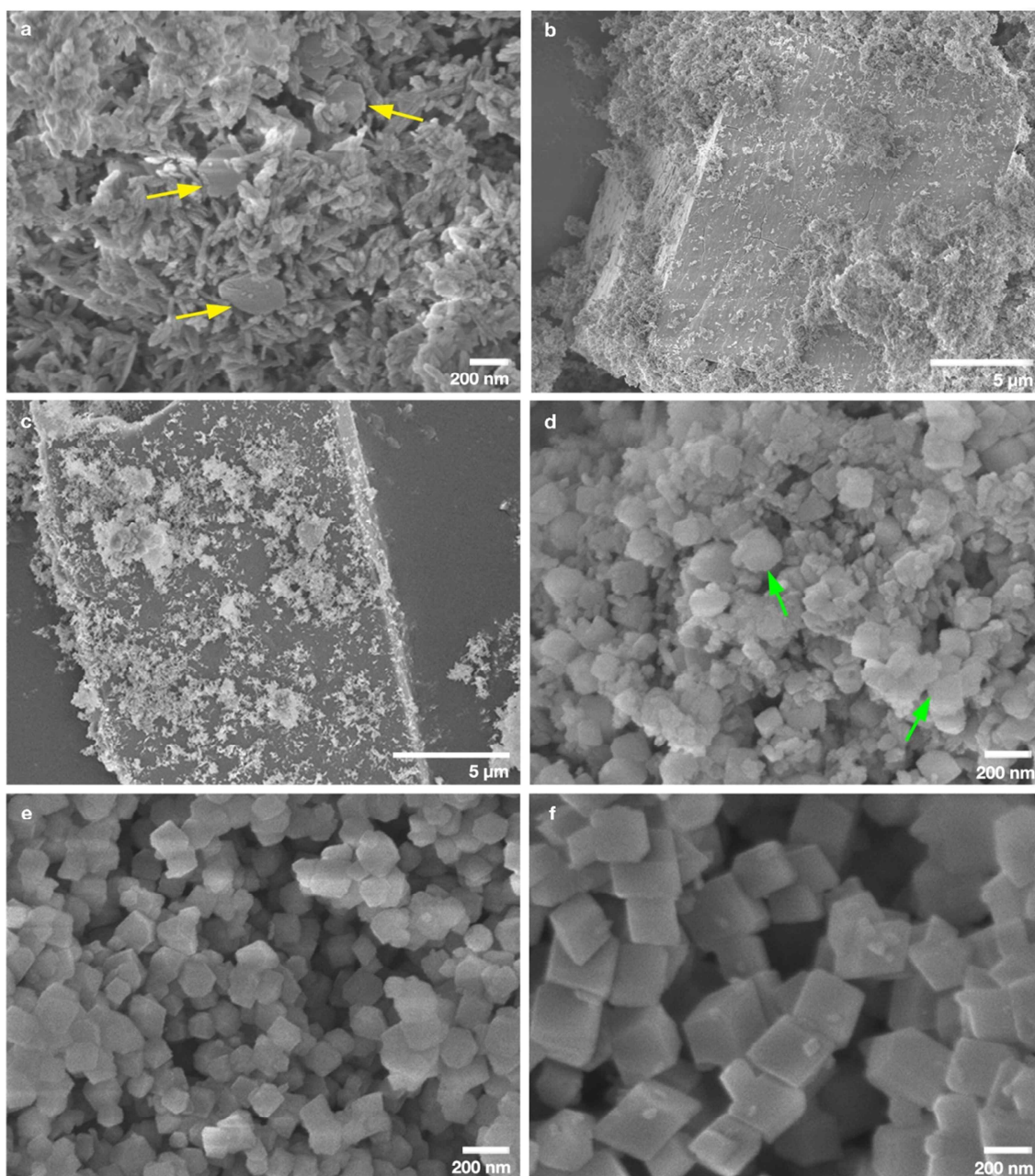


**Figure 6.** FESEM images of the intermediate precipitants collected during the synthesis of whitlockite (WH:  $\text{Ca}_{18}\text{Mg}_2(\text{HPO}_4)_2(\text{PO}_4)_{12}$ ). (a) Stage I. Rice shaped hydroxyapatite (HAP:  $\text{Ca}_{10}(\text{PO}_4)_6(\text{OH})_2$ ) nanoparticles and polygonal platelet shaped  $\text{Mg}(\text{OH})_2$  were observed together on the nanometer scale.  $\text{Mg}(\text{OH})_2$  platelets are indicated by the yellow arrow. (b) Stage II. Cuboid-like dimagnesium phosphate (MP:  $\text{MgHPO}_4$ ) crystals were formed on the micrometer scale. At the surface of the MP crystals, rice shaped HAP nanoparticles existed. (c) Stage III. A large platelet shape of dicalcium phosphate dehydrate (DCPD:  $\text{CaHPO}_4 \cdot 2\text{H}_2\text{O}$ ) was formed, and rice shaped HAP nanoparticles were observed. (d) Stage IV. The rhombohedral morphology of WH nanoparticles began to appear among rice shaped HAP nanoparticles. WH particles are indicated with green arrows. (e) Stage V. The general shape of the nanoparticles was rhombohedral, which reflected that only the WH phase existed in the system. (f) After 2 weeks of aging at  $65^\circ\text{C}$ , the WH nanoparticles grew to a larger size.

system, the HAP gradually dissolved in the acidic conditions while a rhombohedral shape of WH began to appear. In Figure 6d, we marked the rhombohedral WH nanoparticles, which existed between the remaining HAP nanoparticles, with green arrows. After 24 hours (Figure 6e), only rhombohedral nanoparticles were found in the precipitants, which confirmed that a homogenous phase of WH was obtained. When this

reaction proceeded at a lower temperature ( $65^\circ\text{C}$ ), WH precipitated after 2 weeks and had a larger size than the WH formed at a higher temperature within a short aging time (Figure 6f) because the particle nucleation was slow.

The kinetic mechanism for the precipitation of WH in  $\text{Ca}(\text{OH})_2\text{-Mg}(\text{OH})_2\text{-H}_3\text{PO}_4$  aqueous system is represented in Figure 7. At stage I,  $\text{Ca}(\text{OH})_2$  preferentially reacted with the

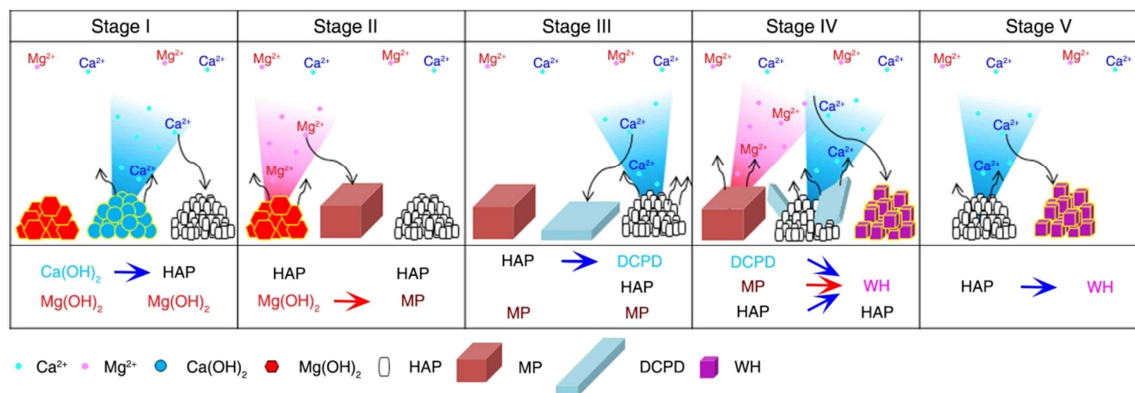


**Figure 7.** Schematic diagram of the intermediate phases that exist in each stage during the precipitation of whitlockite (WH:  $\text{Ca}_{18}\text{Mg}_2(\text{HPO}_4)_2(\text{PO}_4)_{12}$ ) in a  $\text{Ca}(\text{OH})_2$ - $\text{Mg}(\text{OH})_2$ - $\text{H}_3\text{PO}_4$  aqueous system at 70 °C. Calcium ions ( $\text{Ca}^{2+}$ ), magnesium ions ( $\text{Mg}^{2+}$ ), calcium hydroxide ( $\text{Ca}(\text{OH})_2$ ), magnesium hydroxide ( $\text{Mg}(\text{OH})_2$ ), hydroxyapatite (HAP:  $\text{Ca}_{10}(\text{PO}_4)_6(\text{OH})_2$ ), magnesium phosphate (MP:  $\text{MgHPO}_4$ ), dicalcium phosphate dihydrate (DCPD:  $\text{CaHPO}_4 \cdot 2\text{H}_2\text{O}$ ) and WH are presented with graphic symbols as the cyan sphere, pink sphere, red polygon, white ellipse, brown cuboid, sky platelet and purple cuboid, respectively. At each stage, the intermediate phase with a higher solubility dissolves and releases ions to transform into a more stabilized phase.

newly added  $\text{H}_3\text{PO}_4$  to produce HAP. At stage II, after the entire amount of  $\text{Ca}(\text{OH})_2$  was consumed,  $\text{Mg}(\text{OH})_2$  began to react with the newly incorporated  $\text{H}_3\text{PO}_4$  to produce MP. At stage III, after the entire amount of  $\text{Mg}(\text{OH})_2$  was used, HAP transformed into DCPD, which is the favored calcium phosphate phase in acidic conditions. After the entire amount of  $\text{H}_3\text{PO}_4$  was added, DCPD, MP and HAP began to dissolve and transform into WH. At stage V, after the entire amount of resident HAP dissolved, only the WH phase existed in the system. Therefore, the Ca-related compounds and Mg-related compounds had different kinetic paths that each separately reacted with the newly incorporated  $\text{H}_3\text{PO}_4$  to transform into more stabilized phases according to the surrounding environment. For Ca-related compounds,  $\text{Ca}(\text{OH})_2$  reacted with  $\text{H}_3\text{PO}_4$  to form HAP at stage I, which later turned into DCPD in acidic conditions at stage III. In contrast,  $\text{Mg}(\text{OH})_2$  reacted with  $\text{H}_3\text{PO}_4$  to form MP at stage II. Although Ca- and Mg-related compounds existed separately during the kinetic pathway, all of the Ca, Mg and P precipitated into the most stable form of WH at the final stage.

To compare the content of Mg in the precipitants at different experimental times, we analyzed the ratio between Ca and Mg in the precipitants using inductively coupled plasma (ICP) spectroscopy. Before the reaction started, the molar percentages of Ca and Mg were 77% and 23%, respectively. Immediately after the total addition of  $\text{H}_3\text{PO}_4$  into the  $\text{Ca}(\text{OH})_2$ - $\text{Mg}(\text{OH})_2$  solution, the molar percentages of Ca and Mg in the precipitant changed into approximately 96% and 4%, respectively. In addition, the ratio of total cation (Ca+Mg) to anion (P) was 1.5991. Based on these ratios, we calculated the molar ratios between initial phases of MP:DCPD:HAP as 1:3:11.7, using the premise that magnesium is difficult to incorporate inside of DCPD and HAP. Finally, when only the WH phase existed in the system, the molar percentages of Ca and Mg were 90% and 10%, respectively.

In addition, to observe the transition of the residual amount of ions in the system, we conducted ion chromatography analysis on separate filtrates at different experimental times, and the concentrations of the free ion states of  $\text{Ca}^{2+}$  and  $\text{Mg}^{2+}$  in the filtrate were measured. Immediately after the total addition

of  $\text{H}_3\text{PO}_4$ , the free ion states of  $\text{Mg}^{2+}$  and  $\text{Ca}^{2+}$  existed at approximately 2940 ppm and 1076 ppm, respectively. Therefore, excessive  $\text{Mg}^{2+}$  ions were present on the outside of the initial precipitants. Then, as the phase transformed into WH, the concentration of  $\text{Mg}^{2+}$  decreased to 808 ppm, and the concentration of  $\text{Ca}^{2+}$  decreased to 604 ppm. Increased loss of  $\text{Mg}^{2+}$  in solution indicates that  $\text{Mg}^{2+}$  ions were incorporated into the newly formed WH structure from the outer system. In addition, the overall decrease of  $\text{Ca}^{2+}$  demonstrates that the solubility of WH in acidic conditions is lower than the solubility of HAP in neutral conditions. Taken together, the HAP phase that initially formed above neutral pH conditions dissolved and released  $\text{Ca}^{2+}$  and  $\text{PO}_4^{3-}$  ions in the proton rich environment. Then, a pure phase of WH was precipitated due to its strong stability in acidic conditions.

In Figure 8a, based on the experimental data, we present a diagram of the kinetic precipitation pathway of WH depending on the temperature. The intermediate phases formed after the complete addition of all of the starting materials for WH are shown according to the aging time. When the temperature of the system was above 80 °C, only HAP and WH existed immediately after the entire amount of  $\text{H}_3\text{PO}_4$  was added to the system. The pure WH phase was obtained within 12 and 6 hours of aging at 80 °C and 90 °C, respectively. Therefore, as the temperature of the system increased, the kinetic transformation from HAP to WH occurred faster in the  $\text{Ca}(\text{OH})_2$ - $\text{Mg}(\text{OH})_2$ - $\text{H}_3\text{PO}_4$  aqueous system. In contrast, when the temperature of the system was lower, more detailed observation of intermediate phases was possible. At 70 °C, mixture phases of DCPD, MP and HAP existed immediately after the entire amount of  $\text{H}_3\text{PO}_4$  was added to the system. After sufficient aging time, the DCPD and MP phases transformed into WH by priority, and then HAP also turned into WH. Therefore, we confirmed that WH had a higher thermodynamic stability than DCPD and MP, which were previously known as generally stable phases in acidic conditions for Ca- and Mg-phosphate compounds, respectively.

Based on the established kinetic pathway for the precipitation of WH, to confirm that HAP can directly transform into WH, we aged pure HAP nanoparticles with an

additional amount of  $Mg^{2+}$  in acidic conditions, which was set at the level to synthesize WH, at 90 °C for 3 days. The result showed that a portion of the HAP directly turned into a heterogeneous phase of WH (Figure 7b). This partial transform reflects that WH has a higher stability than HAP in acidic conditions.

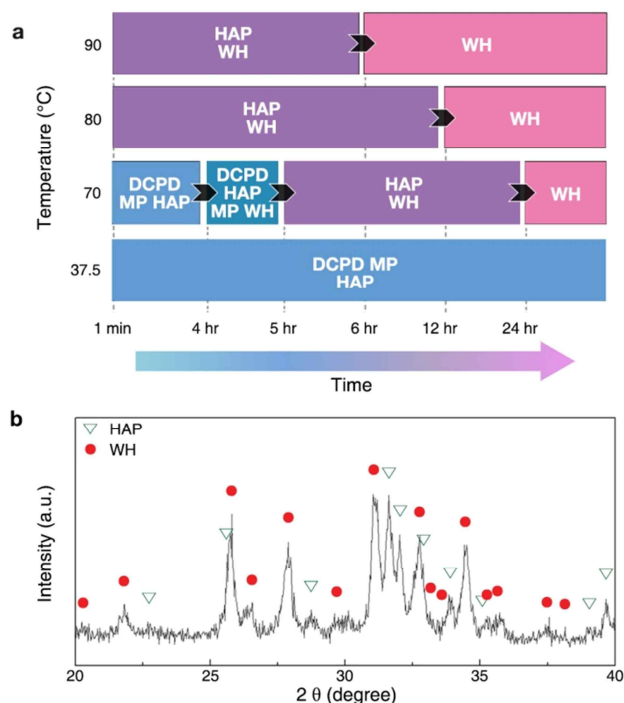


**Figure 8.** Kinetic precipitation pathway of WH. (a) The precipitation pathway of whitlockite (WH:  $Ca_{18}Mg_2(HPO_4)_2(PO_4)_{12}$ ) in a  $Ca(OH)_2$ - $Mg(OH)_2$ - $H_3PO_4$  aqueous system, depending on different temperatures and aging times. (b) The phase transformation of hydroxyapatite (HAP:  $Ca_{10}(PO_4)_6(OH)_2$ ) into WH. The direct phase transformation from HAP to WH was partially observed after aging HAP in acidic conditions with excessive amounts of  $Mg^{2+}$  at 90 °C for 3 days. Peaks corresponding to each phase of HAP and WH in XRD data are marked as the green triangle and red circle, respectively.

Once WH is produced in the *in vivo* system, it would be exposed to the neutral environment where HAP is more stable and more likely to be precipitated. In this regard, an interesting future study can be to investigate the phase transformation between WH and HAP in the *in vitro* system that involves cellular interactions. Additionally, the study of stimulating effects on the surface of WH, which can induce different protein/cell interactions compared with that of HAP, will be another important topic to understand hard tissue and to apply in practical fields.

## Experimental section

Whitlockite (WH:  $Ca_{18}Mg_2(HPO_4)_2(PO_4)_{12}$ ) was synthesized by precipitation with calcium hydroxide ( $Ca(OH)_2$ , 99.0%, High Purity Chemical, Japan), magnesium hydroxide ( $Mg(OH)_2$ , 95.0%, Junsei Chemical Co., Japan) and phosphoric acid ( $H_3PO_4$ , 85.0%, Junsei Chemical Co., Ltd) in an aqueous system. To begin, 0.77 M of  $Ca(OH)_2$  and 0.23 M of  $Mg(OH)_2$

was homogeneously mixed in 500 mL of distilled water at 70 °C using an overhead stirrer (MSM-1 Jeio tech). After 1 hour of stirring, 500 mL of a 0.95 M  $H_3PO_4$  aqueous solution was added to the  $Ca(OH)_2$ - $Mg(OH)_2$  solution dropwise at a speed of 12.5 mL/min using a digital burette (Metrohm 876, Dosimat Plus) and while vigorously stirring. Other possible ratios of starting materials using  $Ca(OH)_2$ ,  $Mg(OH)_2$  and  $H_3PO_4$  for synthesizing a pure phase of WH are indicated in Figure 1a. The precipitants were aged for 24 hours, collected using a filter press and lyophilized. Hydroxyapatite (HAP:  $Ca_{10}(PO_4)_6(OH)_2$ ) was synthesized using a sonochemistry-based precipitation method.  $Ca(OH)_2$  (1.00 M) was initially stirred vigorously in 500 mL of distilled water using an overhead stirrer for 1 hour at room temperature.  $H_3PO_4$  (0.60 M, 500 mL) was added dropwise into the  $Ca(OH)_2$  solution with speed of 12.5 mL/min using a digital burette. During the entire reaction, sonication was provided to achieve complete mixing of the starting materials and to prevent the formation of nonstoichiometric HAP. The precipitants were aged for 24 hours, filter-pressed and lyophilized to obtain dried HAP powder.

The atomic structures in each unit cell of WH and HAP were drawn using CrystalMaker software (Crystal Maker Software Ltd., Oxford, England ([www.crystallmaker.com](http://www.crystallmaker.com))) and were based on the previously reported crystal structure databases of WH and HAP.<sup>25, 30</sup> To analyze the crystal phase of WH, HAP, and the intermediate phases during the precipitation of WH, X-ray diffraction (XRD, M18XHF-SRA, MAC Science Co.) with monochromatic Cu K $\alpha$  radiation ( $\lambda = 1.5405 \text{ \AA}$ ) was used. The intermediate precipitants were rapidly collected from the  $Ca(OH)_2$ - $Mg(OH)_2$ - $H_3PO_4$  solution using a syringe, filter pressed and lyophilized. Field emission scanning electron microscopy (FESEM, JSM-6330F, JEOL) was used to observe the overall morphologies of the final products of WH and HAP and the intermediate precipitants during the precipitation of WH. The individual shape and interplanar spacing of the synthesized WH nanoparticles were examined using high-resolution transmission electron microscopy (HRTEM, JEM-3000F, JEOL). To measure the pH change during the precipitation of WH, during the dropwise addition of  $H_3PO_4$  into the  $Ca(OH)_2$ - $Mg(OH)_2$  solution, the electrode of a pH meter (Schott, Lab860) was fixed in the  $Ca(OH)_2$ - $Mg(OH)_2$  solution and the pH change was recorded. To compare the ratios of Ca and Mg in the precipitant depending on the reaction time, precipitants were collected 1 minute and 24 hours after the addition of the total amount of  $H_3PO_4$  into the system, respectively, and analyzed using an inductive coupled plasma optical emission spectrometer (ICP-OES, Varian 720-ES). To measure the amount of free ions of  $Ca^{2+}$  and  $Mg^{2+}$  in the system, the filtrate was separated through a 0.22  $\mu\text{m}$  membrane filter (Millipore, Durapore) at each experimental time and examined using ion chromatography (Dionex, ICP-3000, USA).

## Conclusions

In this study, by investigating the kinetic pathway of precipitation of WH, we showed that two major phases of bone, HAP and WH, have different stabilities according to the pH level. HAP was precipitated in neutral pH regions, whereas WH was formed in acidic regions with the incorporation of  $Mg^{2+}$  ions. Our finding suggested that WH in bone might be generated from locally formed acidic pH conditions and further indicated that bone is stable in a broad range of pH levels. In addition, the phase transformation between HAP and WH due to pH change demonstrated that human hard tissue is more than

a static support of the body and the mineral itself can act as a dynamic living material that constantly transforms into the proper phase. We expect that discoveries in this study will contribute in the understanding of biomineralization in natural hard tissue and in the design and fabrication of phase transformable biomaterials, especially those related to pH.

### Acknowledgements

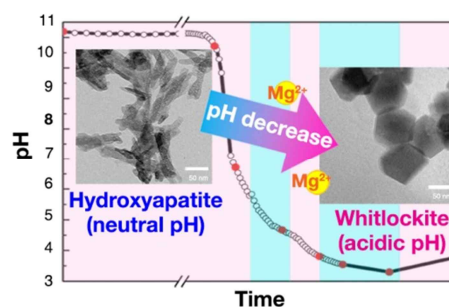
This research was supported by the Basic Science Research Program through the National Research Foundation of Korea (NRF), funded by the Ministry of Science, ICT & Future (No. Grant Number: 2011-0011225); the Global Frontier R&D Program on Center for Multiscale Energy System funded by the National Research Foundation under the Ministry of Science, ICT & Future, Korea (0420-20130104); the International Research & Development Program of the National Research Foundation of Korea (NRF), funded by the Ministry of Science, ICT & Future Planning (No. 2013K1A3A1A32035536).

### Notes and references

Biomolecular Nanomaterials Laboratory, Department of Materials Science and Engineering, Seoul National University, Seoul 151-744, Korea. E-mail: nkitae@snu.ac.kr

1. F. C. M. Driessens and R. M. H. Verbeeck, *Biominerals*, CRC Press: Boca Raton, FL, 1990.
2. J. C. Elliott, *Structure and Chemistry of the Apatites and Other Calcium Orthophosphates*, Elsevier Science & Technology: Amsterdam, 1994.
3. R. Lagier and C. A. Baud, *Pathol. Res. Pract.*, 2003, **199**, 329-335.
4. C. A. Scotchford, M. Vickers and S. Yousuf Ali, *Osteoarthritis Cartil.*, 1995, **3**, 79-94.
5. Y. Hayashi, *J. Electron Microsc.*, 1996, **45**, 501-504.
6. J. Palamara, P. P. Phakey, W. A. Rachinger and H. J. Orams, *Arch. Oral. Biol.*, 1980, **25**, 715-725.
7. D. K. Meinke, H. C. W. Skinner and K. S. Thomson, *Calcif. Tissue Int.*, 1979, **28**, 37-42.
8. P. Quint, J. Althoff, H. Höhling, A. Boyde and W. Laabs, *Calcif. Tissue Int.*, 1980, **32**, 257-261.
9. H. L. Jang, K. Jin, J. Lee, Y. Kim, S. H. Nahm, K. S. Hong and K. T. Nam, *ACS Nano*, 2013, **8**, 634-641.
10. R. LeGeros, G. Daculsi, R. Kijkowska and B. Kerebel, *Magnesium in Health and Disease*, John Libbey: New York, 1989, 11-19.
11. R. Zapanta LeGeros, *Prog. Cryst. Growth Charact. Mater.*, 1981, **4**, 1-45.
12. S. Rowles, *Bull. Soc. Chim. Fr.*, 1968, **1968**, 802.
13. E. Hayek and H. Newesely, *Monatsh. Chemie*, 1958, **89**, 88-95.
14. M. Knuutila, R. Lappalainen and V. Kontturi-NÄRhi, *Eur J Oral Sci*, 1980, **88**, 513-516.
15. G. Nancollas, B. Tomazic and M. Tomson, *Croat. Chem. Acta*, 1976, **48**, 431-438.
16. O. R. Trautz, Zapantal.R and J. P. Legeros, *J. Dent. Res.*, 1964, **43**, 751-754.
17. C. S. Martens and R. C. Harriss, *Geochim. Cosmochim. Acta*, 1970, **34**, 621-625.
18. M. Okazaki, J. Takahashi and H. Kimura, *Caries Res.*, 1986, **20**, 324-331.
19. W. P. Rothwell, J. S. Waugh and J. P. Yesinowski, *J. Am. Chem. Soc.*, 1980, **102**, 2637-2643.
20. J. A. S. Bett, L. G. Christner and W. K. Hall, *J. Am. Chem. Soc.*, 1967, **89**, 5535-5541.
21. A. Osaka, Y. Miura, K. Takeuchi, M. Asada and K. Takahashi, *J. Mater. Sci. Mater. Med.*, 1991, **2**, 51-55.
22. A. Śalósarczyk, E. Stobierska, Z. Paszkiewicz and M. Gawlicki, *J. Am. Ceram. Soc.*, 1996, **79**, 2539-2544.
23. L. Stipniece, K. Salma-Ancane, N. Borodajenko, M. Sokolova, D. Jakovlevs and L. Berzina-Cimdina, *Ceram. Int.*, 2014, **40**, 3261-3267.
24. P. Koutsoukos, Z. Amjad, M. B. Tomson and G. H. Nancollas, *J. Am. Chem. Soc.*, 1980, **102**, 1553-1557.
25. C. Calvo and R. Gopal, *Am. Miner.*, 1975, **60**, 120-133.
26. R. Terpstra and F. Driessens, *Calcif. Tissue Int.*, 1986, **39**, 348-354.
27. W.-H. Zhu, J.-J. Ke, H.-M. Yu and D.-J. Zhang, *J. Power Sources*, 1995, **56**, 75-79.
28. H. McDowell, T. Gregory and W. Brown, *J. Res. Nat. Bur. Stand. A*, 1977, **81**, 273-281.
29. C. Henrist, J. P. Mathieu, C. Vogels, A. Rulmont and R. Cloots, *J. Cryst. Growth*, 2003, **249**, 321-330.
30. J. M. Hughes, M. Cameron and K. D. Crowley, *Am. Miner.*, 1989, **74**, 870-876.

### The table of contents



Whitlockite ( $\text{Ca}_{18}\text{Mg}_2(\text{HPO}_4)_2(\text{PO}_4)_{12}$ ), the second most abundant biomineral in bone, can precipitates from hydroxyapatite ( $\text{Ca}_{10}(\text{PO}_4)_6(\text{OH})_2$ ), the major phase in bone.